Journal of Pharmaceutical Sciences 110 (2021) 239-250

Contents lists available at ScienceDirect

Journal of Pharmaceutical Sciences

journal homepage: www.jpharmsci.org

Pharmaceutics, Drug Delivery and Pharmaceutical Technology

Proteomics-Informed Identification of Luminal Targets For In Situ Diagnosis of Inflammatory Bowel Disease

Shno Asad [a, f], Christine Wegler [b, c, f], David Ahl [d], Christel A.S. Bergström [b, e], Mia Phillipson [d], Per Artursson [b], Alexandra Teleki [a, *]

[a] Department of Pharmacy, Science for Life Laboratory, Uppsala University, SE-75123 Uppsala, Sweden
[b] Department of Pharmacy, Uppsala University, SE-75123 Uppsala, Sweden
[c] Department of Pharmacy, Uppsala University Drug Optimization and Pharmaceutical Profiling Platform (UDOPP), SE-75123 Uppsala, Sweden
[d] Department of Medical Cell Biology, Uppsala University, SE-75123 Uppsala, Sweden
[e] The Swedish Drug Delivery Center, Department of Pharmacy, Uppsala University, SE-75123 Uppsala, Sweden

ARTICLE INFO

Article history:
Received 20 August 2020
Revised 1 November 2020
Accepted 2 November 2020
Available online 4 November 2020

Keywords:
Biomarker(s)
Caco-2 cells
Colon
Gastrointestinal tract
Inflammatory bowel disease (IBD)
In vitro model(s)
Nanoparticle(s)
Principal component analysis
Proteomic
Targeted drug delivery

ABSTRACT

Inflammatory bowel disease (IBD) is a chronic condition resulting in impaired intestinal homeostasis. Current practices for diagnosis of IBD are challenged by invasive, demanding procedures. We hypothesized that proteomics analysis could provide a powerful tool for identifying clinical biomarkers for non-invasive IBD diagnosis. Here, the global intestinal proteomes from commonly used *in vitro* and *in vivo* models of IBD were analyzed to identify apical and luminal proteins that can be targeted by orally delivered diagnostic agents. Global proteomics analysis revealed upregulated plasma membrane proteins in intestinal segments of proximal- and distal colon from dextran sulfate sodium-treated mice and also in inflamed human intestinal Caco-2 cells pretreated with pro-inflammatory agents. The upregulated colon proteins in mice were compared to the proteome of the healthy ileum, to ensure targeting of diagnostic agents to the inflamed colon. Promising target proteins for future investigations of non-invasive diagnosis of IBD were found in both systems and included Tgm2/TGM2, Icam1/ICAM1, Ceacam1/CEACAM1, and Anxa1/ANXA1. Ultimately, these findings will guide the selection of appropriate antibodies for surface functionalization of imaging agents aimed to target inflammatory biomarkers *in situ*.

Introduction

Today, the life-long treatment and diagnosis of inflammatory bowel disease (IBD) suffers from several challenges. There is no standardized diagnostic method available for intestinal inflammation and the current gold standard is endoscopy combined with mucosal biopsies, which is costly, invasive and time-consuming. Disease activity is characterized by symptoms of diarrhea, urgency of defecation, and occasionally rectal bleeding and abdominal pain. IBD is diagnosed based on these clinical symptoms together with endoscopic and histopathologic examinations. However, especially in patients with Crohn's disease (CD), the disease can progress without these symptoms or they can have other causes than an active inflammation. This can result in repeated invasive examinations and in unnecessary or not optimal treatments.[1] Thus, the accurate assessment of disease location and activity is essential for successful disease management, minimizing adverse effects from medication, the risk of relapse, or even development of cancer.[2]

Due to the disadvantages of current means of diagnosing IBD, there is a continued interest in complimentary, non-invasive diagnostic alternatives. These include imaging techniques like computed tomography (CT) or magnetic resonance imaging (MRI)[1,3] and biomarker analyses in feces or serum samples.[4] C-reactive protein (CRP) is a widely used serum indicator for IBD in the clinic. However, it lacks specificity and sensitivity for inflammation in the gastrointestinal tract (GIT), and is only used

Abbreviations: CD, Crohn's disease; CT, computed tomography; DAI, disease activity index; DSS, dextran sulfate sodium; GIT, gastrointestinal tract; H&E, hematoxylin and eosin; IBD, inflammatory bowel disease; IEC, intestinal epithelial cell; LPS, lipopolysaccharide; MRI, magnetic resonance imaging; MS, mass spectrometry; PBS, phosphate-buffered saline; PC, principal component; ROS, reactive oxygen species; SPION, superparamagnetic iron oxide nanoparticle; UC, ulcerative colitis; WT, wild-type.

* Corresponding author. Department of Pharmacy, Science for Life Laboratory, Uppsala University, Box 580, SE-75123 Uppsala, Sweden.
E-mail address: alexandra.teleki@scilifelab.uu.se (A. Teleki).
[f] These authors contributed equally.

https://doi.org/10.1016/j.xphs.2020.11.001

complimentary to other diagnostic methods.[5] To assess disease activity, the upregulated fecal biomarkers of inflammation, neutrophil-associated proteins calprotectin, lactoferrin, and myeloperoxidase, are routinely used in compliment to endoscopic examinations in the clinic.[4] These fecal biomarkers are typically stable in stool for up to one week at room temperature, making them ideal for simple screening in the clinic.[6] However, they do not give any spatial information about the spread of the disease in the GIT and suffer from large interpatient variability.[3] Also, calprotectin is not only a biomarker for IBD but can be associated with e.g. neoplasia, infections, and celiac disease,[4] and is elevated in patients taking nonsteroidal anti-inflammatory drugs.[7] Finally, fecal biomarkers might not comprise a sensitive tool to evaluate early stages of inflammation.[6] In contrast, local, membrane-bound biomarkers on intestinal epithelial cells (IECs) can be targeted to determine the exact disease location in the GIT. Furthermore, local detection of secreted, luminal biomarkers circumvent the stability requirement in stool samples. This could open for novel, potential biomarker targets and improve early detection of intestinal inflammation.

Amongst the non-invasive imaging techniques, CT is currently the preferred practice in hospitals mostly due to its rapid scan time, widespread availability and high resolution. However, it exposes patients to cumulative ionizing radiation as frequent re-evaluation of disease activity is typically required for IBD patients. MRI is thus gaining popularity, especially with the development of advanced MRI methods. Molecular MRI uses contrast agents such as functionalized superparamagnetic iron oxide nanoparticles (SPION) targeting overexpressed disease biomarkers to image disease location *in vivo*. This technique has so far primarily been applied for preclinical cancer diagnosis, as well as imaging of inflammation in the brain.[8] Furthermore, MRI can be employed for the quantitative determination of the local biomarker concentration *in vivo* and this is already explored in clinical trials for cancer monitoring.[9]

In order to develop such non-invasive, *in situ* imaging-based diagnostic tools for IBD, appropriate local biomarker targets have to be identified. Proteomics analysis is a powerful tool in biomarker discovery and has previously been applied for IBD using human tissue biopsies, serum, and feces samples,[10] but to a much lesser extent to understand which structures to target for non-invasive imaging and oral drug delivery. In order to empower preclinical development of such novel targeted imaging probes, biomarker identification has to be carried out initially in commonly used *in vitro* and *in vivo* experimental models of acute inflammation and later on linked with biopsies from patient cohorts.

Several experimental models have been developed to advance the understanding of IBD and thereby developing improved diagnostic and therapeutic platforms. The most commonly used animal model of IBD employs enteral administration of dextran sulfate sodium (DSS) at ~40 kDa in mice to gradually induce epithelial damage, predominantly in the proximal and distal parts of the colon, and resembles ulcerative colitis (UC) in humans.[11,12] Amongst *in vitro* methods, Caco-2 cells originating from human epithelial colorectal adenocarcinoma cells, are widely used in studies of intestinal cell physiology and drug transport.[13] Various methods have been reported to induce inflammation in this cell model and most commonly a mixture of cytokines and lipopolysaccharides (LPS)[14] or DSS[15] is used.

In this study, the global proteomes of the most commonly used experimental *in vitro* and *in vivo* IBD models were quantified with the focus to find biomarkers for *in situ* targeting. The aim was to identify *i)* commonly expressed apical plasma membrane biomarkers on IECs *in vitro* and *in vivo* and *ii)* secreted biomarkers *in vivo*. Our studies identify luminal and membrane-bound IBD biomarkers that will be further investigated as non-invasive targets for diagnosis of IBD.

Experimental

Mouse Model for Acute Colitis

All animal experiments were approved by the Swedish Laboratory Animal Ethical Committee in Uppsala (animal experiment number C6/16) and were conducted in accordance with guidelines of the Swedish National Board for Laboratory Animals. Male, C57BL6/J mice (Taconic M&B, Ry, Denmark and Charles River, Sulzfeld, Germany) weighing between 20 and 35 g before treatment were kept under standardized conditions at a temperature of 21−22 °C and with 12 h light and 12 h dark cycle. For proteomics, fifteen mice were randomly divided into two groups: control (n = 8) and DSS-treated (n = 7). For immunohistochemical analysis, 12 mice were divided into two groups: control (n = 6) and DSS-treated (n = 6). Colitis was induced by adding 3% (w/v) DSS (molecular weight ~40 kDa) to the drinking water for 7 days (Fig. 1a). The colitis progression was evaluated for each DSS-treated mouse (n = 7 for proteomics and n = 6 for immunostaining) by daily assessment of clinical parameters (weight loss, stool consistency, and blood content). It is presented as a disease activity index (DAI) score with a minimum of 0 and maximum of 4 (Fig. S1).[16] At the end of the experiment, the mice were euthanized by isoflurane inhalation followed by cervical dislocation.

Tissue Biopsy Sampling for Proteomics

Intestinal sections of ileum and colon were removed separately and placed in oxygenated Krebs solution. The tissues were rinsed from stool and a midline incision was made longitudinally along the intestine. The tissues were pinned on a Sylgard-lined Petri dish with the luminal side facing down. A fine incision was made through the muscle layer, and muscle was then carefully removed from the underlying tissue. The tissue preparations of the whole ileum were snap frozen in liquid nitrogen, while the preparations of the large intestine were first cut into two segments, proximal colon and distal colon, before snap frozen in liquid nitrogen. The proximal colon was morphologically distinct from the remaining parts of the tissue by transverse folds that project into the lumen. All tissue biopsies were kept at −80 °C until further treatment and analysis.

Immunohistochemistry

Colon tissue was removed and opened longitudinally, rinsed with cold PBS and rolled according to the Swiss-roll technique.[17] Excised tissues were immediately fixed in 4% formalin (Sigma-Aldrich, St. Louis, MO, USA) overnight and then transferred to 70% ethanol in PBS. The tissue preparations were embedded in histowax (Histolab Products AB, Askim, Sweden). Consecutive sections, 4 μm thick, were cut, placed on SuperFrost Plus slides (Thermo Scientific, Braunschweig, Germany) and baked at 52 °C for 45 min. Sections were stained with the following antibodies: rabbit anti-mouse annexin A1 (abcam, #ab214486, dilution. 1:2000), rabbit anti-mouse CEACAM1 (SinoBiological, #50571-R030, dilution 1:500), rabbit anti-mouse ICAM1 (abcam, #ab179707, dilution 1:1000) and rabbit anti-mouse transglutaminase 2 (abcam, #ab109200, dilution 1:100). Shortly, sections were deparaffinised and rehydrated. Antigen retrieval was performed in PT-Link (Agilent, Santa Clara, CA) at 97 °C for 20 min with Envision FLEX Target Retrieval Solution, High pH (Agilent). Staining was performed in Autostainer Link 48 (Agilent) using Envision FLEX+, High pH Kit (Agilent) using goat anti-rabbit immunoglobulins/HRP (Agilent, #P0448, dilution 1:200) as secondary antibody. Slides were counterstained with Mayers Hematoxylin (Histolab Products AB) for 5 min, washed in tap water, dehydrated in sequential changes of alcohols and xylene and mounted with Pertex (Histolab Products AB). All stained

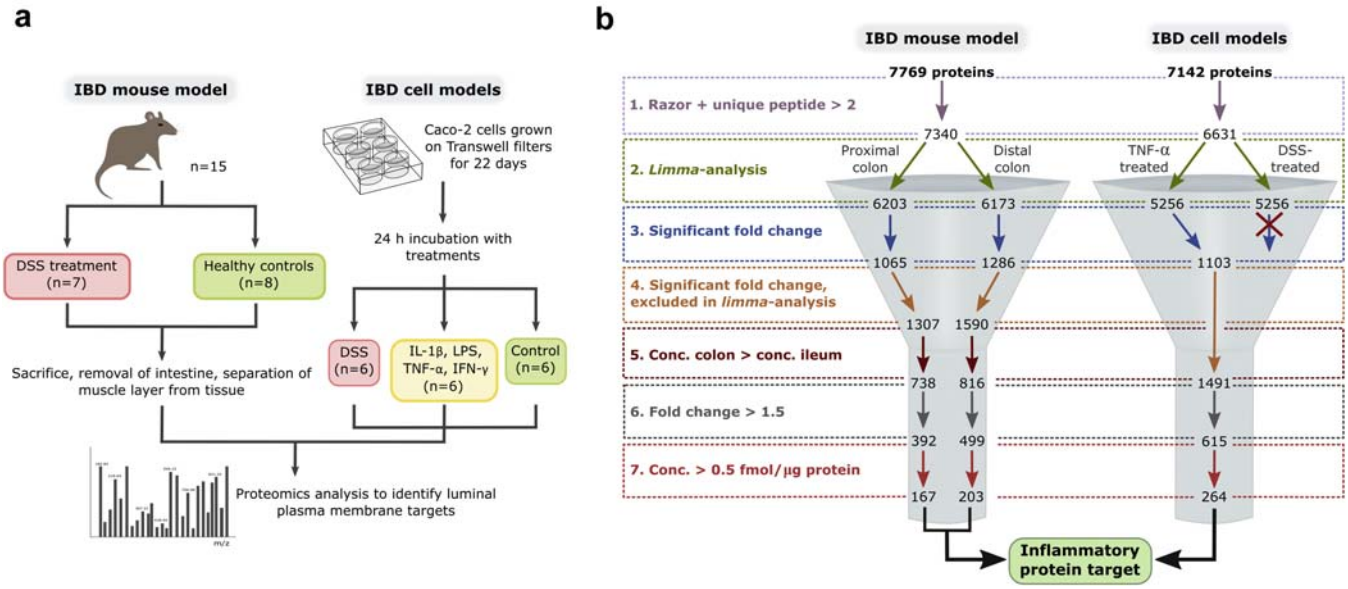

Fig. 1. Treatment of experimental *in vivo* and *in vitro* IBD models to achieve acute inflammation and workflow for the selection of target proteins. (a) Workflow for global proteomics of inflammatory mouse and Caco-2 cell models. Mice (WT, male, C57BL6/J) were treated with DSS in their drinking water for seven days. Intestinal biopsies were collected from ileum, proximal and distal colon. Filter-grown Caco-2 cells were treated with DSS or a mixture of inflammatory agents. (b) Selection criteria to identify plasma membrane bound target proteins in IBD mouse model and TNF-α treated Caco-2 cell model.

specimens were imaged by light microscopy using Axio Scan.Z1 (objective: Plan-Apochromat 20×/0.8 M27; Zeiss, Jena, Germany).

Inflammatory Cell Models

Caco-2 cells (originally obtained from the American Type Culture Collection), passage 96, were maintained in Dulbecco's modified Eagle's medium, containing 10% (v/v) fetal bovine serum, and 1% (v/v) nonessential amino acids. The cells were cultured in an incubator at 37 °C, 10% CO_2 (MMM Group, Munich, Germany) while maintained in 75 cm^2 tissue culture flasks. Cells were seeded on Transwell polycarbonate filters (Corning, NY, USA; diameter 12 mm, pore size 0.4 µm) at a density of 0.5 × 10^6 cells/filter and maintained in Dulbecco's modified Eagle's medium with 10% fetal bovine serum, 1% nonessential amino acids, 100 U/mL penicillin, and 100 µg/mL streptomycin prior to the experiment. All cell culture media and reagents were purchased from ThermoFisher Scientific (Waltham, MA, USA) or Sigma-Aldrich (St. Louis, MO, USA). After 22 days in culture, the cells were treated with filter-sterilized (0.45 µm) solutions of either 1 w/v% dextran sulfate sodium (DSS)[15] or a mixture of inflammatory mediators with tumor necrosis factor (TNF)-α (50 ng/ml), interleukin (IL)-1β (25 ng/ml), lipopolysaccharides (LPS; 10 ng/ml) and interferon (IFN)-γ (50 ng/ml)[14] in culture medium (Fig. 1a). This mixture will simply be referred to as TNF-α treatment in the following. For DSS-treated cells, the medium was added to the apical side of the Transwell filters, while for the cells treated with the TNF-α mixture, the medium was applied to the basolateral side. After 24 h, filters were washed with phosphate-buffered saline (PBS) and then excised and prepared for proteomics analysis. Four 12-well filters were pooled for one sample. In total, six control, six TNF-α and six DSS-treated samples were prepared.

Global Proteomics Analysis

Mouse ileum (DSS-treated: 176 ± 28 mg, control: 158 ± 39 mg), proximal (DSS-treated: 93 ± 24 mg, control: 93 ± 31 mg) and distal (DSS-treated: 60 ± 12 mg, control: 50 ± 16 mg) colon samples were homogenized with a T10 Basic homogenizer (IKA®-Werke GmbH & Co. KG, Staufen, Germany) in lysis buffer containing 2% (w/v) SDS, 50 mM DTT, and 100 mM Tris/HCl, pH 7.8. Caco-2 cells were lysed directly with the lysis buffer. Proteins were denatured at 95 °C and DNA were sheared with a rod sonicator. Proteins were cleaned and digested with the multi-enzyme digestion filter-aided sample preparation (MED-FASP) protocol, using LysC and trypsin.[18] Peptides were desalted on stage-tips packed with C18-material (3 M), and eluted with 60% acetonitrile (ACN) in water.[19,20] Protein and peptide amounts were determined based on tryptophan fluorescence.[21] Peptides were separated on a 50 cm EasySpray C18 column (2 µm particle size, 75 µm inner diameter, ThermoFisher Scientific, Waltham, MA, USA) and eluted with a gradient of 2−25% mobile phase B (0.1% formic acid in 100% ACN) at a flow rate of 300 nL/min over 100 min. This was followed by 15 min elution from 25 to 50% mobile phase B and a final washout of 95% mobile phase B. Peptides were ionized with electrospray in positive mode and analyzed on a Q Exactive HF mass spectrometer (ThermoFisher Scientific, Waltham, MA, USA) using a data-dependent mode with survey scans acquired at 240,000 resolution with maximum ion injection time of 20 ms. Up to the top 15 most abundant isotope patterns with charge ≥2 from the survey scan were selected with an isolation window of 1.4 m/z and fragmented by HCD with normalized collision energies of 28.5. The MS/MS scans were obtained at 15,000 resolution and maximum ion injection time of 60 ms. The resulting MS data were processed with MaxQuant (version 1.6.10.43),[22] where proteins were identified by searching MS and MS/MS data of peptides against the mouse UniProtKB (UP000000589) or human (Caco-2 cells) UniProtKB (UP000005640). Spectral raw intensities were normalized with variance stabilization (vsn),[23] and subsequently used to calculate the protein concentrations using the Total Protein Approach.[24]

Data Analysis and Bioinformatics

To improve the quality of the data analysis, only proteins that were identified with at least two unique + razor peptides from

the MaxQuant processing were subject to further analysis. Proteins with significantly different concentration levels in the treated compared to control sample types were identified with *limma* (in R/Bioconductor),[25] which is an analysis approach that uses linear models to analyze differential expression across all proteins in the dataset. From *limma*-analysis, proteins with absolute concentration fold change (geometric mean concentration treated/control) > 2 and p-value < 0.05 in treated against control samples were considered for further pathway analysis. Functional annotation clustering was performed in R with the clusterProfiler-package[26] searching against the mouse or human database, respectively.

Upregulated plasma membrane bound proteins that can be targeted from the luminal side in the GIT for *in situ* diagnosis of IBD, were identified following the procedure outlined in Fig. 1b. First, only proteins identified with at least two unique + razor peptides were selected (Fig. 1b, step 1). Second, only proteins without missing values in any sample were selected (Fig. 1b, step 2). Next, proteins with a significant fold change (p-values < 0.05 from limma-analysis; Fig. 1b, step 3) in treated compared to healthy controls were selected for further analysis. As *limma*-analysis does not account for missing values, the proteins which were found to be upregulated in the treated mice and cells, but essentially absent in the controls, were manually added to the selection of proteins (Fig. 1b, step 4). Significant fold changes for these proteins were calculated with *t*-test corrected for multiple comparisons with the Holm-Sidak method in GraphPad Prism (version 8.4.0). Additionally for the mouse proteome, proteins with a higher concentration in the treated colon than in the healthy ileum were chosen (Fig. 1b, step 5). This decision was made since inflammation in the mouse model primarily occurs in the colon. Thus, an imaging probe should primarily be targeted there and not bind prematurely in the small intestine. Subsequently, upregulated proteins with a concentration fold change (geometric mean concentration treated/control) $\geq$ 1.5 (Fig. 1b, step 6) in proximal and distal colon were selected. Finally, to ensure sufficient protein concentration for targeting, only proteins with geometric mean concentration $\geq$0.5 fmol/μg total protein (Fig. 1b, step 7) were considered. The subcellular location of these proteins was determined based on their UniProt annotation.

Results

Global Proteomics Analysis of Mouse Model For Acute Colitis

The DSS treatment effectively induced intestinal inflammation in mice, evident by their weight loss and blood in the stool. The decrease in body weight started after five days of DSS treatment with a mean decrease of 7% before sacrifice. After seven days of treatment, the mean DAI score was 2.6 ± 0.5 and 2.1 ± 0.5 (standard deviation) out of maximum 4 across the DSS-treated mice used for proteomics and immunostaining, respectively (Fig. S1). When the tissue samples were collected, shortening of the colon was visually measured from treated mice compared to the healthy controls. Hematoxylin and eosin (H&E)-stained sections of the DSS-treated colon revealed inflammatory morphological changes of the mucosa compared to the healthy controls (Fig. 2). Regional differences were observed as the DSS-induced colitis induced immune cell infiltration, damaged epithelium and altered crypt morphology in the distal colon (Fig. 2c–e), while the proximal region of the colon was unaltered (Fig. 2f).

The global proteomics analysis resulted in quantification of 7340 proteins with at least two unique + razor peptides in total across the ileum, proximal and distal colon samples obtained from all mice (Fig. 1b, step 1, Data S1). The protein concentrations in the ileum were only affected to a small extent by the DSS-treatment compared to those in the healthy mice (Fig. 3a). Principal component analysis (PCA) showed that only 16% of the variability along the second most influential component in the ileum proteomes was explained by the treatment (Fig. S2a). Largest proteome variability was observed in the proximal and distal colon in DSS-treated mice compared to healthy controls (Fig. 3a). In these colon segments 22% and 25% of the variability (along the first most influential component), respectively, was ascribed to changes in the colon tissue from DSS-treated mice (Fig. S2b and S2c). *limma*-analysis showed that the concentrations of 128 proteins were significantly changed (fold change of geometric mean concentration treated/control > 2 and p-value < 0.05) in the ileum after DSS-treatment (Fig. 3b), while this number increased to 257 and 437 proteins in the proximal and distal colon, respectively (Fig. 3b). A correlation in concentration fold changes (geometric mean concentration treated/control) of the proteins quantified in the proximal and distal colon from treated and control mice were found (Pearson's correlation coefficient, r = 0.55), suggesting that both tissue segments were similarly affected by the DSS-treatment (Fig. 3c). Functional annotation clustering confirmed that the significantly changed protein concentrations in the distal and proximal colon were involved in inflammatory response processes, such as 'defense response' and 'immune response' (Fig. 3d). More specifically, proteins involved in these processes with the highest upregulation in both distal and proximal colon of the DSS-treated mice, were S100a9, Lcn2, Chil3, and Iigp1, with concentration fold changes ranging from 26 to 119 (Data S1). No enrichment of biological processes was identified for the affected proteins in the ileum from the treated mice. This further demonstrates that DSS-treatment had a lower impact on the ileum compared to the colon segments.

Global Proteomics Analysis of Inflammatory Caco-2 Cell Models

In the treated and control Caco-2 cells, a total of 6631 proteins were quantified with at least two unique + razor peptides in MaxQuant (Fig. 1b, step 1, Data S1). The largest change in the Caco-2 proteome was observed after the TNF-α treatment, which accounted for 25% of the variability (on the first influential component in the PCA; Fig. 4a). The TNF-α treatment of Caco-2 cells resulted in 465 proteins with significantly changed concentrations. The affected proteins were similarly involved in inflammatory response processes (Fig. 4c) as observed in the colon segments from DSS-treated mice (Fig. 3d). In the TNF-α treated Caco-2 cells, 'defense response' and 'response to cytokine' were the most enriched functional annotation clusters, including proteins such as WIPI2, PARP9, IGBP1, and LRSAM1 with concentrations upregulated 2–4 fold (Data S1). DSS-treatment did not affect the proteome of the Caco-2 cells to the same extent as the TNF-α mixture. For the former, only 105 proteins were significantly changed, and no enriched functional clusters were obtained. Therefore, only TNF-α treated Caco-2 cells were analyzed for luminal protein targets (Fig. 1b).

Selection of Inflammatory Target Proteins

The selection criteria shown in Fig. 1b were applied to identify inflammatory biomarkers for *in situ* colon targeting in the selected experimental IBD models. The filtering process yielded 167 and 203 targets in the proximal (Table S1) and distal colon (Table S2) of the DSS-treated mice, respectively (Fig. 1b, step 7). In the Caco-2 cells, 264 targets were identified (Table S3; Fig. 1b, step 7). Finally, out of the proteins found from the overall filtering process (Fig. 1b, steps 1–7), plasma membrane bound proteins on the apical side of

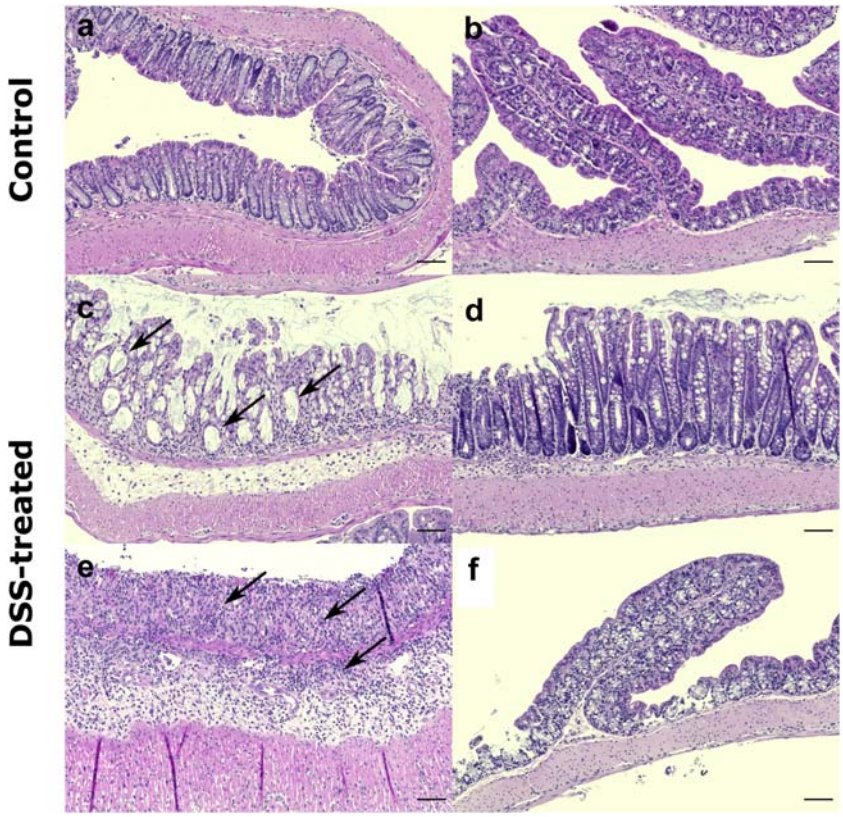

Fig. 2. Representative H&E-stained colon sections from healthy and DSS-treated mice (scale bar: 20 μm). (a) Distal and (b) proximal colon of healthy control with an intact and ordered epithelium. (c) Distal colon of DSS-treated mouse displaying irregular crypts with variable diameter along the depth of single crypts or dilated crypts containing mucus, indicated by arrows. (d) Epithelial cell hyperplasia appears as elongation of crypts in the colon. (e) Complete loss of crypts and infiltration of immune cells demonstrates a severe inflammatory state (arrows indicate neutrophils). (f) Proximal colon of DSS-treated mouse shows no evident morphological changes compared to healthy controls.

epithelial cells (Table 1) and secreted proteins in the lumen (Table 2), based on their UniProt annotations, are proposed here as *in situ* targets.

A large number of the identified membrane bound proteins were associated with immune cells (Table 2) in agreement with the functional annotation clustering (Fig. 3d). Examples of such upregulated proteins in both proximal and distal colon are Lcn2 (80.1 and 26.3-fold, respectively), Prtn3 (17.7 and 11.0-fold, respectively) and Cybb (4.0 and 4.9-fold, respectively). The latter, however, was found at similar concentrations in both ileum and colon (0.4 fmol/μg and 0.6–0.7 fmol/μg respectively). Elane was also highly upregulated in the proximal colon (56.6-fold). This protein was also found at moderate concentrations in the distal colon (geometric mean: 0.5 fmol/μg), while it was not detectable in the healthy tissue. Thus, p-value and fold change could not be determined for this protein in the distal colon.

Plasma membrane bound proteins, common between the selected mouse and cell models (Table 1), are of particular interest for preclinical development of diagnostic agents to enable rapid translation and facile correlation between *in vitro* and *in vivo* models. Thus, proteins located on the apical side of the intestinal epithelium were selected. In total, four upregulated proteins present in both *in vitro* and *in vivo* models were found: Tgm2/TGM2, Icam1/ICAM1, Ceacam1/CEACAM1, and Anxa1/ANXA1 (Table 1). These proteins were all upregulated during inflammation in the experimental IBD models, with the exception of Icam1 that was only upregulated in the distal colon and slightly downregulated in the proximal colon. It should be noted, that the selection criteria for each protein in terms of fold change and total protein concentration (Fig. 1b) were never met for all samples analyzed, i.e. Caco-2 cells, distal and proximal colon segments. However, data was included in Table 1 if the criteria were met in at least one of these samples. For example, in the Caco-2 cells the highest upregulation was obtained for Icam1 (48-fold), with only a moderate increase in the distal colon for this protein (1.3-fold) and even a decrease in the proximal colon (0.7-fold). Tgm2/TGM2 and Ceacam1/CEACAM1 met all selection criteria in the Caco-2 cells (3.5 and 3.6-fold respectively) as well as the distal colon (2.4 and 1.6-fold, respectively). These proteins were more strongly upregulated in the treated samples in the distal colon as compared to the proximal colon (1.3 and 1.2-fold, respectively). In contrast, Anxa1/ANXA1 had a higher fold change in the proximal (1.8-fold) compared to distal colon (1.4-fold). It was also upregulated in the Caco-2 cells (2.3-fold), however, at overall rather low total protein concentration (geometric mean < 0.5 fmol/μg even after TNF-α treatment).

Importantly, expression of the four protein targets Tgm2, Icam1, Ceacam1, and Anxa1 was confirmed using immunohistochemistry in both inflamed (Fig. 5) and healthy mouse tissue, which is in agreement with the proteomics results (Table 1). While Anxa1 was moderately expressed along the crypts of nearly intact epithelial cells in the distal colon (Fig. 5a), it was not detected in highly inflamed areas that exhibited complete crypt loss (Fig. S3a and S3b). Ceacam1 was highly expressed along the epithelial cell surface in both distal (Fig. 5b) and proximal colon (Fig. 5f), but, similarly to Anxa1, was not observed in the inflamed regions with complete crypt loss (Fig. S3c and S3d). In contrast, Icam1 was highly expressed in such highly inflamed areas (Fig. 5c), while it was not observed in areas with less inflammation and more intact

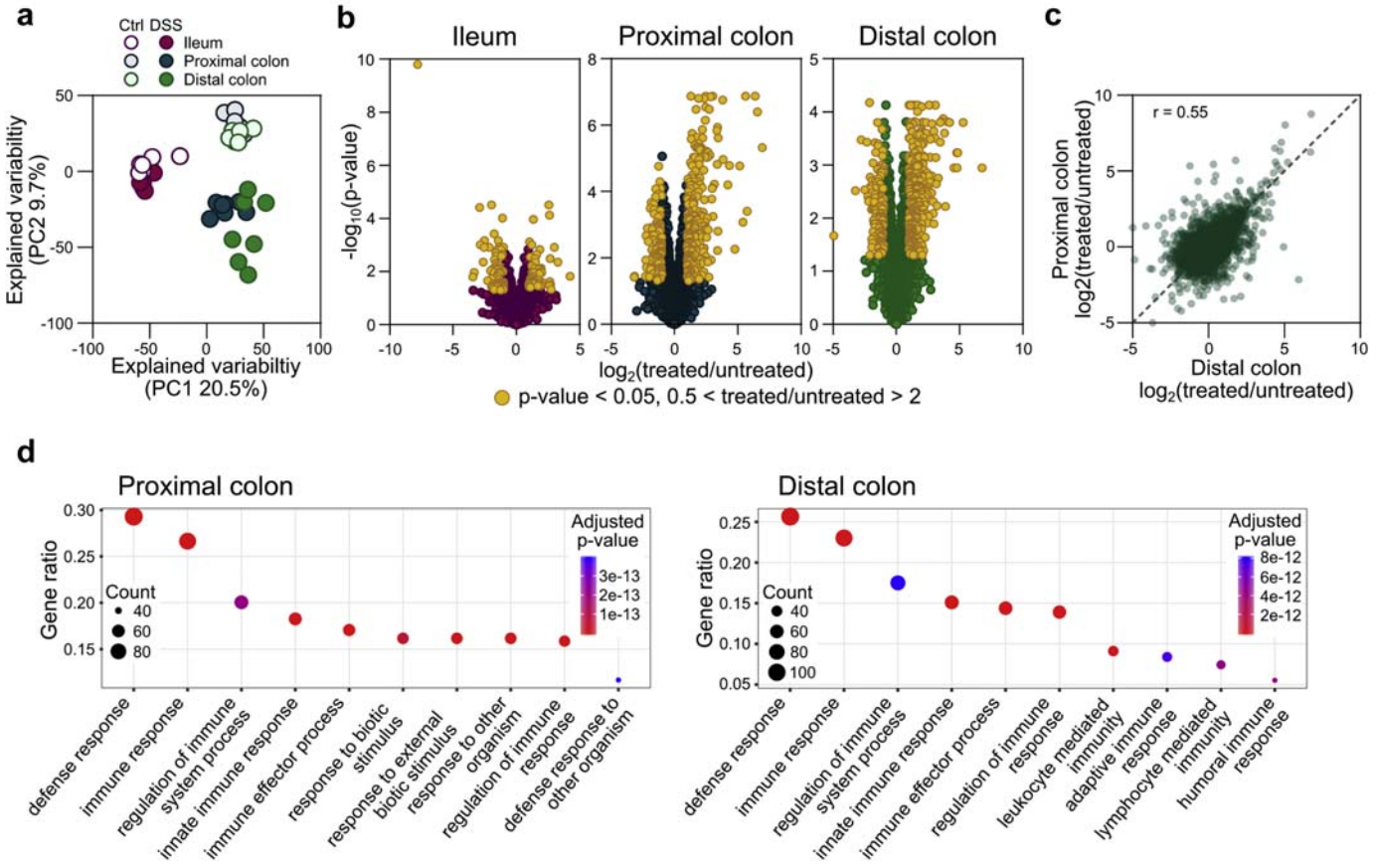

Fig. 3. Proteomics analysis of ileum, proximal and distal colon samples from healthy (n = 8) and DSS-treated mice (n = 7). (a) Principal component (PC) analysis of protein concentrations in ileum, proximal and distal colon samples. (b) Protein concentration fold change from treated and healthy mice against p-values, as calculated from *limma*-analysis, in ileum, proximal and distal colon samples. (c) Correlation of protein concentration fold change between treated and healthy mice in distal and proximal colon from DSS-treated mice. (d) Enriched biological processes from significantly changed proteins in proximal and distal colon from DSS-treated mice.

epithelium (Fig. S3e and S3f). Tgm2 was primarily found in the muscle layer and lamina propria, however, the expression of Tgm2 close to the IEC surface increased in severely inflamed regions (Fig. 5d).

Discussion

To develop novel, non-invasive diagnostic tools for IBD, relevant biomarkers have to be identified. This can be achieved by using proteomics analysis of tissue biopsies from patients, as well as from experimental *in vitro* and *in vivo* IBD models important for preclinical development. Here, global proteomics was used to study the protein expression in a wild-type (WT)-mouse model for acute colitis and two types of inflammatory Caco-2 cell models for the first time. With this approach, the total proteome could be quantified and compared across these commonly used experimental IBD models with the goal to select common targets for preclinical development of *in situ* diagnostic probes (Fig. 6).

Inflammatory Response in the Experimental IBD Models

The global proteome of Caco-2 cells was hardly affected by the DSS-treatment (Fig. 4a). This can be explained by the proposed mode of action by DSS to cause intestinal inflammation *in vivo*. As DSS disrupts the intestinal mucus layer, the epithelium is exposed to microbiota in the lumen that trigger the production of pro-inflammatory agents and recruitment of immune cells, ultimately leading to an inflamed state.[11] This process cannot be mimicked by the DSS-treated Caco-2 cell culture that lacks microbiota, blood flow and an immune system. DSS itself can disrupt cell function, and thus previous reports using this treatment have primarily investigated its effect on cytotoxicity, monolayer integrity, and release of pro-inflammatory cytokines.[15,27] In order to more closely mimic the inflammatory processes in the *in vivo* mouse model, the TNF-α treatment of the Caco-2 cells is more applicable as it produces a similar inflammatory response as that in the DSS-treated mice (Figs. 3d and 4c, respectively).

For the colitis mouse model, the DAI score of the treated mice at day seven (Fig. S1) was in line with previous studies,[28–30] demonstrating an effectively induced intestinal inflammation. This inflammation causes release of proteases, free radicals and metalloproteinases, and results in colon shortening,[31] as also observed in this study. The inflamed state of the DSS-treated mice was confirmed by immunohistochemistry of colon tissue (Fig. 2). DSS-induced colitis was confirmed when comparing colon tissues from the healthy controls (Fig. 4a and b) with the DSS-treated mice (Fig. 2c–f), as the latter revealed altered epithelial morphology with less ordered crypts (Fig. 2c), variable diameters in adjacent crypts or complete crypt loss. Furthermore, certain regions of the DSS-treated colon also exhibited elongated crypts (hyperplasia; Fig. 2d) that can be attributed to intestinal inflammation[32] along with highly increased infiltration of immune cells between the crypts (Fig. 2e). These morphological changes were only observed in the distal colon, while the proximal colon was unaltered (Fig. 2f).

DSS-treatment has been shown to cause inflammation by disrupting the epithelium mostly in the distal colon.[29,33] This is in

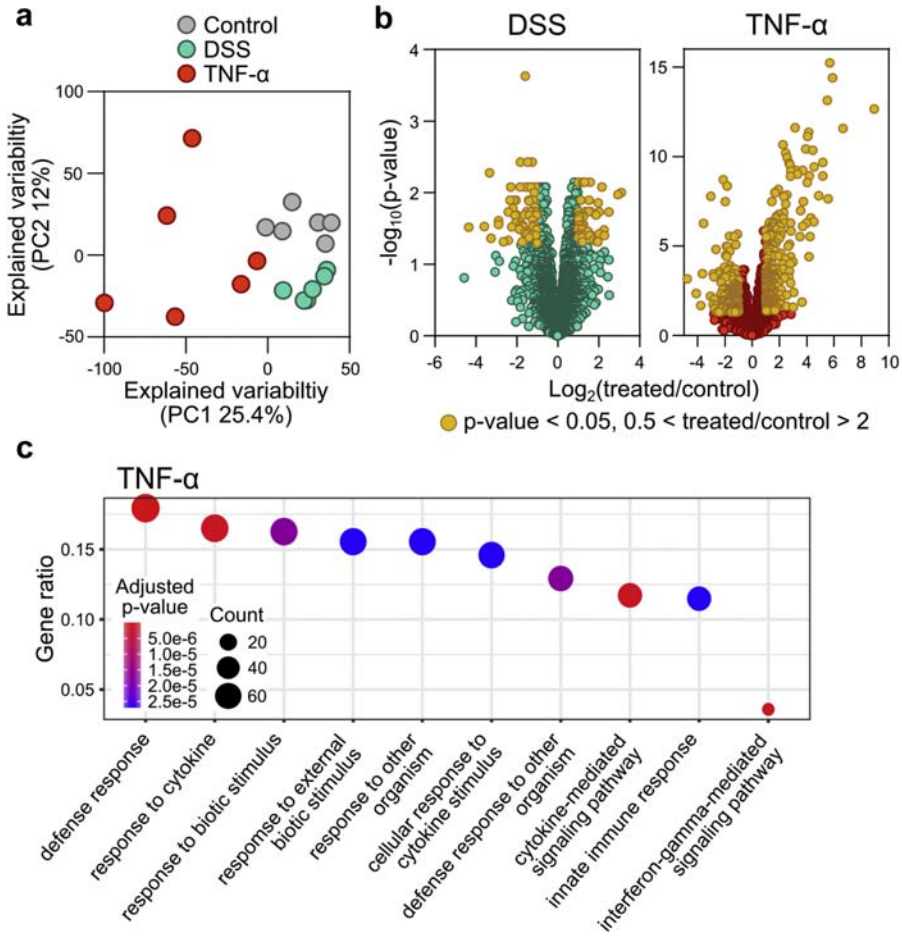

Fig. 4. Proteomics analysis of control (n = 6), DSS (n = 6), and TNF-α treated Caco-2 cells (n = 6). (a) Principal component (PC) analysis of protein concentration in control, DSS, and TNF-α treated Caco-2 cells. (b) Protein concentration fold change between treated and control cells against p-values, as calculated from *limma*-analysis. (c) Enriched biological processes from significantly changed proteins in TNF-α treated Caco-2 cells.

agreement with the small impact of the DSS-treatment on the ileum proteomes (Fig. 3a and b), and specifically proteins involved in inflammatory response, as well as the histomorphological changes in the distal colon sections (Fig. 2c—e). Interestingly, both proximal and distal colon samples showed similar proteome changes (Fig. 3c) and enriched inflammatory response processes (Fig. 3d) after DSS-treatment. For the proximal colon, the discrepancy between the results from immunohistochemistry and proteomics might originate from the difference in sensitivity of these two methods. Proteomics might be more sensitive to pre-inflammatory alterations rather than overt disease facilitating early detection and treatment of IBD. Previous studies have also reported upregulated mRNA levels of pro-inflammatory cytokines in both proximal and distal colon after DSS-treatment, albeit to a higher extent in the distal colon.[34]

The inflamed condition of the mice was further confirmed by the presence of highly upregulated known luminal IBD biomarkers in the proximal and distal colon (Table 2): myeloperoxidase (Mpo), calprotectin (S100a8 and S100a9), lactoferrin (Ltf), and eosinophil protein X (Epx). These biomarkers are routinely used in the clinic for non-invasive diagnosis using feces samples from IBD patients.[4,35] Mpo is a lysosomal protein, secreted from neutrophils to combat invading microbes.[35] Calprotectin is composed of two calcium- and zinc-binding proteins, S100a8 and S100a9 (Table 2). During inflammation, calprotectin is released from immune cells, and can thus be found in feces.[36] Epx is secreted from activated eosinophil granulocytes, and is abundant in the mucosa in active UC and CD.[37,38] Furthermore, the presence of highly upregulated proteins representing different subunits of fibrinogen, Fga, Fgb, and Fgg (with fold changes between 9.9 and 10.6 in proximal colon and 8.1—11.1 in distal colon, respectively; Tables S1 and S2), also indicate an ongoing inflammation in the mice and is in line with high fibrinogen plasma levels reported in IBD patients.[39]

Identification of IEC-Anchored Protein Targets

Plasma membrane proteins expressed commonly on the IECs of DSS-treated mice and inflammation induced Caco-2 cells were identified using the selection criteria shown in Fig. 1b for at least one of the samples. It is not to be expected that the upregulation will be quantitatively similar in the *in vitro* and *in vivo* setting, as the experimental procedure and complexity are different when moving from the *in vitro* to the *in vivo* situation. However, targets that are upregulated in both systems are useful when developing new imaging probes, and to allow contrasting the obtained results to the healthy intestine. The upregulated proteins included Tgm2/TGM2, Icam1/ICAM1, Ceacam1/CEACAM1, and Anxa1/ANXA1 (Table 1). Overexpression of these proteins has previously been reported during active inflammation in IBD patients, confirming the clinical relevance of these biomarkers. Transglutaminase 2 (Tgm2/TGM2, 2.4- and 3.5-fold in distal colon and Caco-2 cells

Table 1
Upregulated Proteins Located Apically in the Plasma Membrane of Caco-2 Cells and Inflamed Intestinal Segments in Mice.

Gene Name	Caco-2			Proximal Colon			Distal Colon			Ileum	Comments
	Fold Change	Conc. TNF-α Treated	Conc. Control	Fold Change	Conc. Treated	Conc. Healthy	Fold Change	Conc. Treated	Conc. Healthy	Conc. Healthy	
Anxa1/ANXA1	2.3	0.4	0.2	1.8	29.7	16.7	1.4	41.7	31.8	8.6	• Annexin A1 • Secreted in intestinal mucosal tissues during inflammation • Release of extracellular vesicles containing annexin A1 from epithelial cells promote mucosal wound repair[44,60]
Ceacam1/CEACAM1	3.6	4.9	1.4	*1.2*	*3.0*	*2.4*	1.6	2.6	1.7	1.9	• Carcinoembryonic antigen-related cell adhesion molecule 5 • Overexpressed on surface of colonic ECs in Crohn's disease[42]
Icam1/ICAM1	48.0	22.8	0.5	*0.7*	*0.6*	*0.8*	*1.3*	*0.3*	*0.2*	0.2	• Intercellular adhesion molecule 1 • Upregulated on apical surface of IECs during inflammation[46,47]
Tgm2/TGM2	3.5	20.2	5.8	*1.3*	*9.4*	*7.4*	2.4	10.6	4.4	9.4	• Transglutaminase 2 • Apoptosis, cell differentiation, inflammation • Upregulated in mucosal layer in IBD[41]

Protein concentrations (fmol/μg protein) were calculated with the Total Protein Approach[24] and are shown as geometric mean values (n = 6 in each group for Caco-2 cells; healthy n = 8, treated n = 7 for mice). Fold change is protein concentration in treated/untreated. Protein expression was not significantly changed for numbers given in italics. The listed proteins are sorted alphabetically.

respectively; Table 1) is widely expressed in the gut mucosa where it is involved in apoptosis, cell differentiation, and inflammation and is upregulated in the GIT tissue of IBD patients.[40,41] Carcinoembryonic antigen-related cell adhesion molecule 1 (Ceacam1/CEACAM1, 1.6- and 3.6-fold in distal colon and Caco-2 cells respectively; Table 1) is an epithelial glycoprotein found on the colonic epithelium surface involved in cell adhesion, signal transduction and innate immunity.[42] Its overexpression has previously been reported in colonic biopsies from patients with active Crohn's disease.[43] Annexin A1 (Anxa1/ANXA1, 1.8- and 2.3-fold in proximal colon and Caco-2 cells respectively; Table 1) is elevated in inflamed tissues of IBD patients as epithelial cells release extracellular vesicles with Anxa1/ANXA1 to promote intestinal mucosal wound repair.[44,45] Thus, the presence of Anxa1 indicates intestinal injury, which subsequently makes it a valuable marker for wound healing, useful for evaluating treatment outcomes. The low concentration of Anxa1 in the healthy ileum compared to the diseased colon segments (Table 1) makes this protein an interesting biomarker for colon targeting. In contrast, Tgm2 and Ceacam1 also show relatively high expression in healthy ileum. Thus, a fraction of orally delivered targeting systems using these protein targets could be consumed in the upstream intestinal region before reaching the affected colon and is expected to contribute with a certain background in the images. Intercellular adhesion molecule 1 (ICAM1) was highly upregulated in the TNF-α treated Caco-2 cells (48-fold, Table 1) and is known to play a central role in IBD pathophysiology, facilitating polymorphonuclear neutrophil adhesion and retention at the apical epithelial membrane in inflamed intestines.[46] It is upregulated on the apical surfaces of IECs during inflammation[47] and has been proposed for GIT targeting of orally delivered nanocarriers.[48] However, in this study, Icam1 was found only moderately upregulated in the distal colon of DSS-treated mice (1.3-fold, $p = 0.32$).

Localization of the identified IEC-anchored protein targets was validated by immunohistochemical staining of colon sections from the DSS-treated mice (Fig. 5). Anxa1 (Fig. 5a and e) and Ceacam1 (Fig. 5b and f) were found across the epithelium of moderately inflamed regions and especially Ceacam1 was strongly expressed on the IEC surface. In contrast, the presence of Icam1 (Fig. 5c and g) and Tgm2 (Fig. 5d and h) was more notable in highly inflamed areas with complete crypt loss. The loss of histomorphological features in these areas could render these proteins accessible for targeting from the luminal side of the GIT. These results indicate that the expression of the identified proteins differ in the various inflammatory states of the GIT, and could be explored further to locally distinguish IBD disease activity. Overall, Tgm2, Ceacam1, and Anxa1 were identified as the most promising inflammatory IEC-anchored protein targets common for the selected *in vitro* and *in vivo* IBD models. These common targets can bridge the gap between cell and mouse models for IBD for the future development of diagnostic systems.

Plasma Membrane Proteins of Immune Cells and Proteins Secreted in the Lumen

The majority of inflammatory proteins in DSS-treated mice is found in immune cells, such as neutrophils, macrophages, and lymphocytes known to infiltrate the mucosa and appear in the intestinal lumen during overt inflammation.[11] This process cannot be mimicked by the *in vitro* Caco-2 cell model. As luminal presence of these proteins is a hallmark of intestinal inflammation, they form less accurate targets for localizing the site of inflammation in the GIT compared to the previously discussed IEC-anchored proteins. However, proteins expressed on or released by immune cells can be used to quantify disease activity. Currently used clinical fecal

Table 2
Proteins Located Extracellularly in Inflamed Intestinal Segments in Mice.

Gene Name	Proximal Colon			Distal Colon			Ileum	Comments
	Fold Change	Conc. Treated	Conc. Healthy	Fold Change	Conc. Treated	Conc. Healthy	Conc. Healthy	
Mpo	76.5	1.9	0.02	105.5	1.1	0.01	0.09	• Myeloperoxidase • Released from neutrophils and macrophages, exhibits antibacterial effects • Increased levels in feces correlate to disease activity in IBD patients[61]
S100a8	265.2	6.4	0.02	33.2	1.6	0.1	0.3	• S100a9 and S100a8: heterodimer calprotectin
S100a9	118.5	31.5	0.3	28.0	11.8	0.4	1.4	• Secreted from immune cells during inflammation • Used as feces marker for IBD[36,62]
Lcn2	80.1	5.5	0.1	26.3	2.3	0.1	0.2	• Lipocalin 2 • Enhances bacterial clearance, prevents development of intestinal inflammation • Increased expression in intestinal tissues of IBD patients[63]
Ltf	91.7	2.8	0.03	20.8	0.9	0.04	1.3	• Lactoferrin • Secreted by neutrophils, exhibits antimicrobial effect • Ltf in feces correlates with severity of GIT inflammation[64]
Ctsg	48.7	0.5	0.01	21.4	0.2	0.01	0.02	• Cathepsin G • Secreted in colonic lumen, triggers inflammation • Increased expression in feces of IBD patients[54–56]
Epx	7.6	4.6	0.6	12.7	3.4	0.3	1.4	• Eosinophil protein X • Released by activated eosinophils, exhibits cytotoxic effects • Elevated concentrations in feces of IBD patients[38]
Prtn3	17.6	0.8	0.04	11.0	0.3	0.03	0.03	• Myeloblastin • Degradation of extracellular proteins at sites of inflammation, delays neutrophil clearance • Potentiates inflammation and autoimmunity[57]
Elane	57.6	0.8	0.08	NA	NA	NA	0.03	• Neutrophil elastase • Mediates inflammation by processing cytokines, chemokines and growth factors • Elevated expression in colonic mucosal biopsies from IBD patients[53]
Cybb	4.0	0.6	0.1	4.9	0.7	0.1	0.4	• Cytochrome *b*-245 (beta chain) • Component of NOX2 that transports electrons from cytoplasmic side to generate ROS[65,66]
Itgb2	5.4	0.9	0.2	4.8	0.8	0.2	0.5	• Integrin β2 receptor • Adhesion, cell communication, migration • Dysregulated during inflammation[67,68]
Mrc1	2.7	0.4	0.2	3.9	0.9	0.2	0.1	• Macrophage mannose receptor 1 • Promotion of antigen presentation[69]
Gsdmdc1	1.4	2.3	1.7	1.7	3.0	1.7	1.8	• Gasdermin-D • Mediator of pyroptosis • Translocates to the plasma membrane, forms pores that induce cell lytic death[70]

Protein concentrations (fmol/μg protein) were calculated with the Total Protein Approach[24] and are shown as geometric mean values (healthy n = 8, treated n = 7 for mice). Fold change is protein concentration in treated/untreated. The listed proteins are sorted with descending fold change in the distal colon.

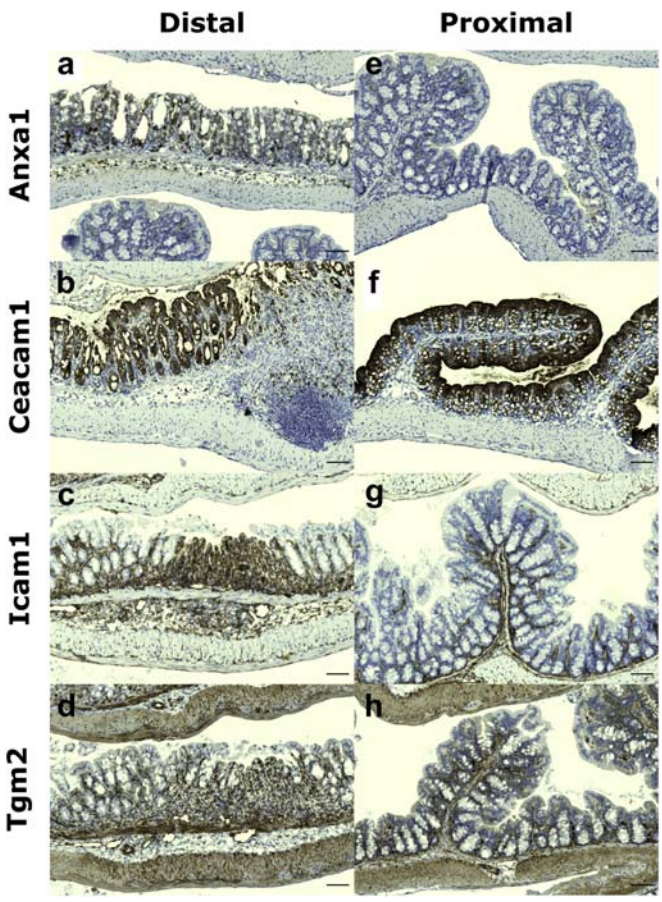

Fig. 5. Immunohistochemically stained distal (left column, a-d) and proximal colon (right column, e-h) sections illustrate localization of protein targets in DSS-treated mice (scale bar: 20 μm). Anxa1 (a, e) and Ceacam1 (b, f) are expressed in moderately damaged epithelial cells, while Icam1 (c, g) and Tgm2 (d, h) show an increased presence in severely inflamed regions of the distal colon.

biomarkers, such as calprotectin and Ltf described previously, have shown good correlation with disease activity,[49] however, due to the harsh conditions of the fecal environment with bacterially expressed proteases, other biomarkers might be subject to cleavage throughout the GIT. Therefore, targeting luminal or immune cell associated proteins *in situ* could still be a promising strategy for diagnosing, localizing, and managing IBD.

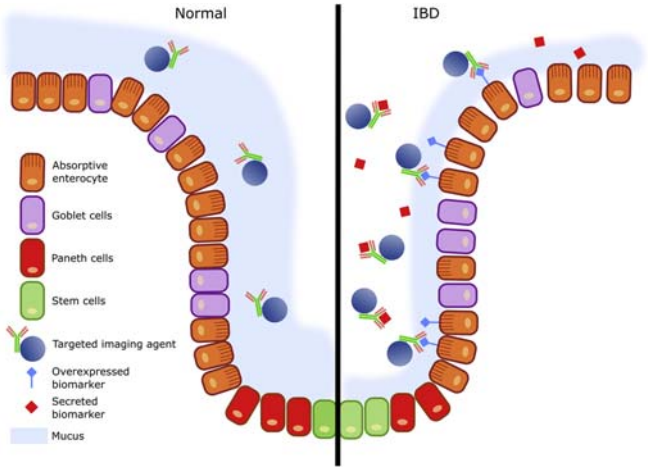

Fig. 6. Schematics of targeted imaging agents functionalized with antibodies binding to upregulated luminal and apical proteins for non-invasive, *in situ* diagnosis of IBD. Figure not drawn to scale.

Apart from these well-known fecal biomarkers, lipocalin 2 (Lcn2), cathepsin G (Ctsg), neutrophil elastase (Elane), and myeloblastin (Prtn3) were also highly upregulated in the inflamed colon segments of the mice (Table 2). Elevated Lcn2 levels have been reported in serum, urine, and feces of IBD patients.[50–52] Elane is a serine protease secreted from neutrophils that has been reported at increased concentration in the colonic mucosa of IBD patients.[53] Ctsg and Prtn3 are both serine proteases. The former is secreted by the colonic mucosa and plays a key role in the pathogenesis of IBD.[54–56] There are not many studies regarding Prtn3 and its role in IBD, however, it is thought to be involved in degradation of extracellular matrix and modulating neutrophil clearance, thereby potentially enhancing inflammation and autoimmunity.[57,58] Finally, Cybb, Itgb2, Mrc1, and Gsdmdc1 were found upregulated at moderate levels compared to the previously mentioned proteins in the inflamed colon tissue from mice and are all linked to inflammatory responses (Table 2).

Overall, the global proteomics approach identified several proteins (e.g. Lcn2, Ctsg, Prtn3 and Elane) that could be explored further as biomarkers for IBD disease activity *in situ* in the GIT. They could thus complement currently used, well-known luminal biomarkers such as calprotectin, Ltf and Mpo that have so far been limited for determining disease activity *ex vivo*. Common for the selected IEC-anchored and secreted proteins is that they can be targeted from the luminal side of the GIT. Thus compared to serum biomarkers, they are specific for intestinal inflammation. In particular, the use of imaging nanoparticles, such as SPION functionalized with antibodies that target the identified biomarkers *in situ*, could be a strategy to provide non-invasive, local and quantitative IBD diagnosis (Fig. 6).

Conclusions

In this work, commonly used *in vitro* and *in vivo* preclinical IBD models were analyzed by global proteomics to identify upregulated inflammatory proteins. We found that Tgm2/TGM2, Ceacam1/CEACAM1, Icam1/ICAM1, and Anxa1/ANXA1 were commonly expressed plasma membrane biomarkers on IECs *in vitro* and *in vivo*. These proteins are thereby promising, clinically relevant targets for development of diagnostic imaging probes that can easily be studied across the different experimental IBD models. Furthermore, highly upregulated, luminal and immune cell-associated proteins in the *in vivo* mouse model could provide quantitative information about IBD disease activity *in situ* in the GIT. Prominent amongst these proteins were Mpo, calprotectin (S100a8 and S100a9), Ltf, and Epx, already well-known from established *ex vivo* feces analyses in the clinic, as well as Lcn2, Prtn3, Elane, and Ctsg. Overall, the provided dataset (Data S1) includes the global proteomes of inflammatory Caco-2 cell and DSS colitis mice models. This can be further used to elucidate common proteins expressed intracellularly for delivery systems intended to pass through the epithelial plasma membrane. In future, the current proteomics approach to develop targeted diagnostic probes could be extended towards other animal disease models for IBD (e.g. intrarectal administration of haptenating agents) and human tissue biopsies from IBD patients.

Acknowledgements

The authors gratefully acknowledge Dr. Svetlana Popova at the laboratory for Clinical Pathology at Uppsala University Hospital for immunohistochemical staining of tissue samples. This work was supported by the Science for Life Laboratory, Sweden. Per

Artursson and Christine Wegler acknowledge funding from the Swedish Research Council (grant numbers 5715 och 1951). Mia Phillipson and David Ahl acknowledge funding from Knut and Alice Wallenberg foundation, Sweden as well as the Swedish Research Council (grant number 2552). The mass spectrometry proteomics data has been deposited to the ProteomeXchange Consortium via the PRIDE[59] partner repository with the dataset identifier PXD020245.

Appendix A Supplementary Data

Supplementary data to this article can be found online at https://doi.org/10.1016/j.xphs.2020.11.001.

References

1. Kilcoyne A, Kaplan JL, Gee MS. Inflammatory bowel disease imaging: current practice and future directions. *World J Gastroenterol*. 2016;22(3):917-932.
2. Olén O, Erichsen R, Sachs MC, et al. Colorectal cancer in ulcerative colitis: a Scandinavian population-based cohort study. *Lancet*. 2020;395(10218):123-131.
3. Cozijnsen MA, Ben Shoham A, Kang B, et al. Development and validation of the mucosal inflammation noninvasive index for pediatric Crohn's disease. *Clin Gastroenterol Hepatol*. 2020;18(1):133-140.e131.
4. Peterson CGB, Lampinen M, Hansson T, Lidén M, Hällgren R, Carlson M. Evaluation of biomarkers for ulcerative colitis comparing two sampling methods: fecal markers reflect colorectal inflammation both macroscopically and on a cellular level. *Scand J Clin Lab Invest*. 2016;76(5):393-401.
5. Chen P, Zhou G, Lin J, et al. Serum biomarkers for inflammatory bowel disease. *Front Med*. 2020;7(123).
6. Tibble J, Teahon K, Thjodleifsson B, et al. A simple method for assessing intestinal inflammation in Crohn's disease. *Gut*. 2000;47(4):506-513.
7. Assche GV. Fecal biomarkers for the diagnosis and management of inflammatory bowel disease. *Gastroenterol Hepatol*. 2011;7(6):396-398.
8. Gauberti M, Montagne A, Quenault A, Vivien D. Molecular magnetic resonance imaging of brain-immune interactions. *Front Cell Neurosci*. 2014;8:389.
9. Daniel KD, Kim GY, Vassiliou CC, et al. Implantable diagnostic device for cancer monitoring. *Biosens Bioelectron*. 2009;24(11):3252-3257.
10. Chan PP, Wasinger VC, Leong RW. Current application of proteomics in biomarker discovery for inflammatory bowel disease. *World J Gastrointest Pathophysiol*. 2016;7(1):27-37.
11. Eichele DD, Kharbanda KK. Dextran sodium sulfate colitis murine model: an indispensable tool for advancing our understanding of inflammatory bowel diseases pathogenesis. *World J Gastroenterol*. 2017;23(33):6016-6029.
12. Kiesler P, Fuss IJ, Strober W. Experimental models of inflammatory bowel diseases. *Cell Mol Gastroenterol Hepatol*. 2015;1(2):154-170.
13. Artursson P. Epithelial transport of drugs in cell culture. I: a model for studying the passive diffusion of drugs over intestinal absorptive (Caco-2) cells. *J Pharm Sci*. 1990;79(6):476-482.
14. Van De Walle J, Hendrickx A, Romier B, Larondelle Y, Schneider Y-J. Inflammatory parameters in Caco-2 cells: effect of stimuli nature, concentration, combination and cell differentiation. *Toxicol In Vitro*. 2010;24(5):1441-1449.
15. Araki Y, Sugihara H, Hattori T. In vitro effects of dextran sulfate sodium on a Caco-2 cell line and plausible mechanisms for dextran sulfate sodium-induced colitis. *Oncol Rep*. 2006;16(6):1357-1362.
16. Cooper HS, Murthy SN, Shah RS, Sedergran DJ. Clinicopathologic study of dextran sulfate sodium experimental murine colitis. *Lab Invest*. 1993;69(2):238-249.
17. Reilly RW, Kirsner JB. Runt intestinal disease. *Lab Invest*. 1965;14:102-107.
18. Wiśniewski JR, Mann M. Consecutive proteolytic digestion in an enzyme reactor increases depth of proteomic and phosphoproteomic analysis. *Anal Chem*. 2012;84(6):2631-2637.
19. Rappsilber J, Ishihama Y, Mann M. Stop and go extraction tips for matrix-assisted laser desorption/ionization, nanoelectrospray, and LC/MS sample pretreatment in proteomics. *Anal Chem*. 2003;75(3):663-670.
20. Wiśniewski JR. Label-free quantitative analysis of mitochondrial proteomes using the multienzyme digestion-filter aided sample preparation (MED-FASP) and "total protein approach". In: Mokranjac D, Perocchi F, eds. *Mitochondria: Practical Protocols*. New York, NY: Springer New York; 2017:69-77.
21. Wiśniewski JR, Gaugaz FZ. Fast and sensitive total protein and peptide assays for proteomic analysis. *Anal Chem*. 2015;87(8):4110-4116.
22. Tyanova S, Temu T, Cox J. The MaxQuant computational platform for mass spectrometry-based shotgun proteomics. *Nat Protoc*. 2016;11(12):2301-2319.
23. Huber W, von Heydebreck A, Sültmann H, Poustka A, Vingron M. Variance stabilization applied to microarray data calibration and to the quantification of differential expression. *Bioinformatics*. 2002;18(suppl_1):S96-S104.
24. Wiśniewski JR, Rakus D. Multi-enzyme digestion FASP and the 'Total Protein Approach'-based absolute quantification of the Escherichia coli proteome. *J Proteomics*. 2014;109:322-331.
25. Ritchie ME, Phipson B, Wu D, et al. Limma powers differential expression analyses for RNA-sequencing and microarray studies. *Nucleic Acids Res*. 2015;43(7):e47.
26. Yu G, Wang L-G, Han Y, He Q-Y. clusterProfiler: an R Package for comparing biological themes among gene clusters. *Omics*. 2012;16(5):284-287.
27. Chang K-W, Kuo C-Y. 6-Gingerol modulates proinflammatory responses in dextran sodium sulfate (DSS)-treated Caco-2 cells and experimental colitis in mice through adenosine monophosphate-activated protein kinase (AMPK) activation. *Food Funct*. 2015;6(10):3334-3341.
28. Lo Sasso G, Phillips BW, Sewer A, et al. The reduction of DSS-induced colitis severity in mice exposed to cigarette smoke is linked to immune modulation and microbial shifts. *Sci Rep*. 2020;10(1):3829.
29. Chassaing B, Aitken JD, Malleshappa M, Vijay-Kumar M. Dextran sulfate sodium (DSS)-induced colitis in mice. *Curr Protoc Immunol*. 2014;104:15.25.11-15.25.14.
30. Park YH, Kim N, Shim YK, et al. Adequate dextran sodium sulfate-induced colitis model in mice and effective outcome measurement method. *J Cancer Prev*. 2015;20(4):260-267.
31. Aw W, Jia H, Lyu W, et al. Integrated omics profiling of dextran sodium sulfate-induced colitic mice supplemented with Wolfberry (Lycium barbarum). *NPJ Sci Food*. 2020;4(1):5.
32. Erben U, Loddenkemper C, Doerfel K, et al. A guide to histomorphological evaluation of intestinal inflammation in mouse models. *Int J Clin Exp Pathol*. 2014;7(8):4557-4576.
33. Biton IE, Stettner N, Brener O, Erez A, Harmelin A, Garbow JR. Assessing mucosal inflammation in a DSS-induced colitis mouse model by MR colonography. *Tomography*. 2018;4(1):4-13.
34. Yan Y, Kolachala V, Dalmasso G, et al. Temporal and spatial analysis of clinical and molecular parameters in dextran sodium sulfate induced colitis. *PLoS One*. 2009;4(6):e6073.
35. Hansberry DR, Shah K, Agarwal P, Agarwal N. Fecal myeloperoxidase as a biomarker for inflammatory bowel disease. *Cureus*. 2017;9(1):e1004.
36. Pruenster M, Vogl T, Roth J, Sperandio M. S100A8/A9: from basic science to clinical application. *Pharmacol Ther*. 2016;167:120-131.
37. Wagner M, Peterson CG, Ridefelt P, Sangfelt P, Carlson M. Fecal markers of inflammation used as surrogate markers for treatment outcome in relapsing inflammatory bowel disease. *World J Gastroenterol*. 2008;14(36):5584-5589. discussion 5588.
38. Saitoh O, Kojima K, Sugi K, et al. Fecal eosinophil granule-derived proteins reflect disease activity in inflammatory bowel disease. *Am J Gastroenterol*. 1999;94(12):3513-3520.
39. Dolapcioglu C, Soylu A, Kendir T, et al. Coagulation parameters in inflammatory bowel disease. *Int J Clin Exp Med*. 2014;7(5):1442-1448.
40. Piacentini M, D'Eletto M, Farrace MG, et al. Characterization of distinct subcellular location of transglutaminase type II: changes in intracellular distribution in physiological and pathological states. *Cell Tissue Res*. 2014;358(3):793-805.
41. Elli L, Ciulla MM, Busca G, et al. Beneficial effects of treatment with transglutaminase inhibitor cystamine on the severity of inflammation in a rat model of inflammatory bowel disease. *Lab Invest*. 2011;91(3):452-461.
42. Roda G, Dahan S, Mezzanotte L, et al. Defect in CEACAM family member expression in Crohn's disease IECs is regulated by the transcription factor SOX9. *Inflamm Bowel Dis*. 2009;15(12):1775-1783.
43. Denmark V, Xu J, Dahan S, Mayer L. CEACAM5 is upregulated with inflammation in Crohn's colitis in response to IL-22: P-207. *Inflamm Bowel Dis*. 2011;17(Suppl_2):S73-S74.
44. Zou Z, Zuo D, Yang J, Fan H. The ANXA1 released from intestinal epithelial cells alleviate DSS-induced colitis by improving NKG2A expression of Natural Killer cells. *Biochem Biophys Res Commun*. 2016;478(1):213-220.
45. Reischl S, Troger J, Jesinghaus M, et al. Annexin A1 expression capacity as a determinant for disease severity in Crohn's disease. *Dig Dis*. 2020;38(5):398-407.
46. Sumagin R, Brazil JC, Nava P, et al. Neutrophil interactions with epithelial-expressed ICAM-1 enhances intestinal mucosal wound healing. *Mucosal Immunol*. 2016;9(5):1151-1162.
47. Reinisch W, Hung K, Hassan-Zahraee M, Cataldi F. Targeting endothelial ligands: ICAM-1/alicaforsen, MAdCAM-1. *J Crohns Colitis*. 2018;12(suppl_2):S669-S677.
48. Ghaffarian R, Herrero EP, Oh H, Raghavan SR, Muro S. Chitosan-alginate microcapsules provide gastric protection and intestinal release of ICAM-1-targeting nanocarriers, enabling GI targeting in vivo. *Adv Funct Mater*. 2016;26(20):3382-3393.
49. Yamamoto T, Shiraki M, Bamba T, Umegae S, Matsumoto K. Faecal calprotectin and lactoferrin as markers for monitoring disease activity and predicting clinical recurrence in patients with Crohn's disease after ileocolonic resection: a prospective pilot study. *United European Gastroenterol J*. 2013;1(5):368-374.
50. Oikonomou KA, Kapsoritakis AN, Theodoridou C, et al. Neutrophil gelatinase-associated lipocalin (NGAL) in inflammatory bowel disease: association with pathophysiology of inflammation, established markers, and disease activity. *J Gastroenterol*. 2012;47(5):519-530.
51. Bolignano D, Della Torre A, Lacquaniti A, Costantino G, Fries W, Buemi M. Neutrophil gelatinase-associated lipocalin levels in patients with Crohn disease undergoing treatment with infliximab. *J Invest Med*. 2010;58(3):569-571.

52. Nielsen OH, Gionchetti P, Ainsworth M, et al. Rectal dialysate and fecal concentrations of neutrophil gelatinase-associated lipocalin, interleukin-8, and tumor necrosis factor-alpha in ulcerative colitis. *Am J Gastroenterol*. 1999;94(10):2923-2928.
53. Anderson BM, Poole DP, Aurelio L, et al. Application of a chemical probe to detect neutrophil elastase activation during inflammatory bowel disease. *Sci Rep*. 2019;9(1):13295.
54. Gao S, Zhu H, Zuo X, Luo H. Cathepsin G and its role in inflammation and autoimmune diseases. *Arch Rheumatol*. 2018;33(4):498-504.
55. Dabek M, Ferrier L, Roka R, et al. Luminal cathepsin G and protease-activated receptor 4: a duet involved in alterations of the colonic epithelial barrier in ulcerative colitis. *Am J Pathol*. 2009;175(1):207-214.
56. Denadai-Souza A, Bonnart C, Tapias NS, et al. Functional proteomic profiling of secreted serine proteases in health and inflammatory bowel disease. *Sci Rep*. 2018;8(1):7834.
57. Csernok E, Gross WL, Radice A, Sinico RA. Chapter 13 - antineutrophil cytoplasmic antibodies with specificity for proteinase 3. In: Shoenfeld Y, Meroni PL, Gershwin ME, eds. *Autoantibodies*. third ed. San Diego: Elsevier; 2014:115-120.
58. Kirov S, Sasson A, Zhang C, et al. Degradation of the extracellular matrix is part of the pathology of ulcerative colitis. *Mol Omics*. 2019;15(1):67-76.
59. Perez-Riverol Y, Csordas A, Bai J, et al. The PRIDE database and related tools and resources in 2019: improving support for quantification data. *Nucleic Acids Res*. 2019;47(D1):D442-D450.
60. Sheikh MH, Solito E. Annexin A1: uncovering the many talents of an old protein. *Int J Mol Sci*. 2018;19(4):1045.
61. Chami B, Martin NJJ, Dennis JM, Witting PK. Myeloperoxidase in the inflamed colon: a novel target for treating inflammatory bowel disease. *Arch Biochem Biophys*. 2018;645:61-71.
62. Chen B, Miller AL, Rebelatto M, et al. S100A9 induced inflammatory responses are mediated by distinct damage associated molecular patterns (DAMP) receptors in vitro and in vivo. *PLoS One*. 2015;10(2):e0115828.
63. Toyonaga T, Matsuura M, Mori K, et al. Lipocalin 2 prevents intestinal inflammation by enhancing phagocytic bacterial clearance in macrophages. *Sci Rep*. 2016;6(1):35014.
64. Dai J, Liu WZ, Zhao YP, Hu YB, Ge ZZ. Relationship between fecal lactoferrin and inflammatory bowel disease. *Scand J Gastroenterol*. 2007;42(12):1440-1444.
65. Singel KL, Segal BH. NOX2-dependent regulation of inflammation. *Clin Sci*. 2016;130(7):479-490.
66. Bedard K, Krause KH. The NOX family of ROS-generating NADPH oxidases: physiology and pathophysiology. *Physiol Rev*. 2007;87(1):245-313.
67. Arnaout MA. Biology and structure of leukocyte β (2) integrins and their role in inflammation. *F1000Res*. 2016;5.
68. Lamb CA, O'Byrne S, Keir ME, Butcher EC. Gut-selective integrin-targeted therapies for inflammatory bowel disease. *J Crohns Colitis*. 2018;12(suppl_2):S653-S668.
69. Martinez-Pomares L. The mannose receptor. *J Leukoc Biol*. 2012;92(6):1177-1186.
70. Ma C, Yang D, Wang B, et al. Gasdermin D in macrophages restrains colitis by controlling cGAS-mediated inflammation. *Sci Adv*. 2020;6(21):eaaz6717.